Available online at www.sciencedirect.com
ScienceDirect
ELSEVIER
Palaeogeography, Palaeoclimatology, Palaeoecology 247 (2007) 382–401
PALAEO
www.elsevier.com/locate/palaeo

The Late Quaternary evolution of water masses in the eastern Indian Ocean between Australia and Indonesia, based on benthic foraminifera faunal and carbon isotopes analyses

Davide S. Murgese *, Patrick De Deckker

Department of Earth and Marine Sciences, The Australian National University, Canberra ACT 0200, Australia

Received 22 September 2005; received in revised form 7 November 2006; accepted 9 November 2006

Abstract

Benthic foraminifera and carbon isotopes from closely spaced samples taken from three deep-sea cores were analysed to reconstruct the palaeoceanographic evolution of the eastern Indian Ocean for the last 30 kyrs, with an extension back to 60 kyrs based on one core.

Benthic foraminifera were studied by means of *Q*-mode Factor Analysis. The benthic foraminifera accumulation rate (BFAR) and the accumulation rates (AR) of *Bulimina aculeata*, *Epistominella exigua* and *Uvigerina proboscidea* were calculated for determining episodes of increased organic matter supply to the sea floor. The $\delta^{18}O$ and $\delta^{13}C$ records of *Cibicidoides wuellerstorfi* were measured from all 3 cores to gather information about past intermediate- and deep-water circulation and changes in sea-surface palaeoproductivity.

The co-variance of the organic matter supply and dissolved-oxygen levels affected the distribution of benthic foraminifera. Below a depth of 1800 m, reduced deep-water circulation was recognised by a low $\delta^{13}C$ of *C. wuellerstorfi* and increased carbon-flux rate by a high BFAR and *B. aculeata*, *E. exigua* and *U. proboscidea* AR, as well as by a *B. aculeata* faunal dominance. A more oligotrophic environment was characterised by a low BFAR and *B. aculeata*, *E. exigua* and *U. proboscidea* AR. Active deep-water circulation was postulated with high $\delta^{13}C$ values for *C. wuellerstorfi* and by a faunal dominance by *C. wuellerstorfi*. At intermediate depths (~1000 m) and south of 20°S, the presence of strong bottom currents and the lateral advection of small amounts of organic matter, favoured the suspension feeder *C. wuellerstorfi*. Under extremely high dissolved-oxygen levels, determined by the increased influence of the Antarctic Intermediate Water (seen through high $\delta^{13}C$ of *C. wuellerstorfi*) and a reduced supply of organic matter, *Nummoloculina irregularis* and *Globocassidulina subglobosa* dominated the benthic foraminifera assemblage. The reduction of oxygen levels, a more stratified water column and the Leeuwin Current flow, along its present pattern, favoured the species *U. proboscidea* and *Bolivina robusta*.

Based on these observations, the following palaeoceanographic evolution of the eastern Indian Ocean is proposed:

- For *60–35 kyr BP*, conditions of higher productivity (compared to the Present) at the sea surface were suggested for the Banda Sea.
- For *35–15 kyr BP*, high productivity still characterised the Banda Sea. Strong and oxygenated bottom currents were present offshore Western Australia. For the Last Glacial Maximum, a reduction of deep-water circulation characterised the eastern Indian Ocean, while more active circulation was recorded at intermediate depths. Productivity also increased offshore the north coast of Western Australia

* Corresponding author.
E-mail address: murgese@seaconsult.it (D.S. Murgese).

doi:10.1016/j.palaeo.2006.11.002

- For *15–5 kyr BP*, a reduction in productivity levels over the Banda Sea is related to increased atmospheric precipitation, which led to the formation of a low-salinity water cap at the sea surface. Off the north coast of Western Australia, productivity levels remained similar to those recorded for the LGM, probably due to the nutrients injected into the sea by rivers. Off the northwest coast of Western Australia, a deepened nutricline prevented any increase of organic matter supply to the sea floor.
- For *5 kyr BP–Present*, in the Banda Sea, productivity levels are similar to the Present. Off the Western Australian coast, an increased influence of the oxygen-depleted Indonesian Intermediate Water and the Leeuwin Current engendered a more stratified water column, characterised by lower dissolved-oxygen levels.

Keywords: Delta 13C; Productivity; Antarctic Intermediate Water; Indian Ocean water masses; *Bulimina aculeata*; South Java Upwelling; Benthic foraminifer accumulation rate; Last Glacial Maximum

1. Introduction

The eastern Indian Ocean is an important region for understanding the mechanisms ruling the global oceanic circulation (Wijffels et al., 1996), in particular the Indonesian Throughflow that sees the transfer of Pacific Ocean water into the Indian Ocean. Already, a large number of oceanographic studies were conducted to describe the oceanic processes that take place in this area (Wyrtki, 1958, 1962; Fieux et al., 1994, 1996; Gordon and Fine, 1996; Wijffels et al., 2002). In addition, the study of the palaeoceanographic evolution for the eastern Indian Ocean during the Late Quaternary represents an important step for reconstructing the environmental modifications that occurred during the past in the region; this may give a better perspective since the instrumental record only spans a few decades. This study aims to improve our knowledge in this respect.

Today, the excess of precipitation over evaporation is responsible for the presence of a low-salinity water cap over the Indo-Pacific Warm Pool region (Tomczak and Godfrey, 1994). Such low-salinity water flows into the eastern Indian Ocean, preventing upwelling to occur off the Western Australian coast (Pearce, 1991) and also reducing the effectiveness of the South Java Upwelling System (Wyrtki, 1962). Studies on pollen transported at sea from land during the past indicate, for the period between 40 and 14 kyr BP, more arid conditions and reduced precipitation over the Australasian region (van der Kaars, 1991; van der Kaars and Dam, 1995, 1997; van der Kaars and De Deckker, 2002; van der Kaars et al., 2006). Under this scenario, sea-surface and intermediate water salinity levels for the Indo-Pacific Warm Pool (called Warm Pool thereafter) region must have been higher (Martinez et al., 1998b) and accompanied by modified intermediate and deep-water circulations (Duplessy et al., 1988, 1989; Rutberg et al., 2000). Consequently, a different scenario would have characterised the eastern Indian Ocean before Marine Isotope Stage 1 (MIS1). Most research from this region has focused on past conditions at the sea-surface (Okada and Wells, 1997; Martinez et al., 1997, 1998a,b; Takahashi and Okada, 2000; Gingele et al., 2001, 2002), and, to some extent, conditions at the sea floor were also examined (Van Marle, 1988, 1989; McCorkle et al., 1994; Wells et al., 1994; Veeh et al., 2000). Results obtained, so far, regarding the palaeoceanographic setting for the eastern Indian Ocean during the Last Glacial Maximum (LGM), suggest a different pattern for the Leeuwin Current accompanied by an increased intensity of the South Java Upwelling System (Martinez et al., 1999; Takahashi and Okada, 2000; Gingele et al., 2001) and increased productivity for the Banda Sea (Spooner et al., 2005). Conflicting results were obtained for offshore the west coast of Western Australia: while Prell et al. (1980) and Wells and Wells (1994) indicated a decreased sea-surface temperature during the LGM, Martinez et al. (1999) suggested no significant temperature variation, at least in the Warm Pool area. The use of different proxies also provided contradictory answers regarding oceanic productivity levels: some (benthic foraminifera accumulation rate, sediment uranium content, $CaCO_3$ mass accumulation rate, benthic foraminifera distribution) would indicate increased productivity (McCorkle et al., 1994; Wells et al., 1994), while others ($\delta^{13}C$ of *Cibicidoides wuellerstorfi*, nannoplankton, planktonic foraminifera) would suggest a situation similar to the present (Okada and Wells, 1997; Martinez et al., 1999). Furthermore, the absence of data related to the sea floor from the Indonesian region does not allow a complete reconstruction of the palaeoenvironments for the entire eastern Indian Ocean. This fragmented picture may hide the explanation for the ambiguous records reported from offshore Western Australia.

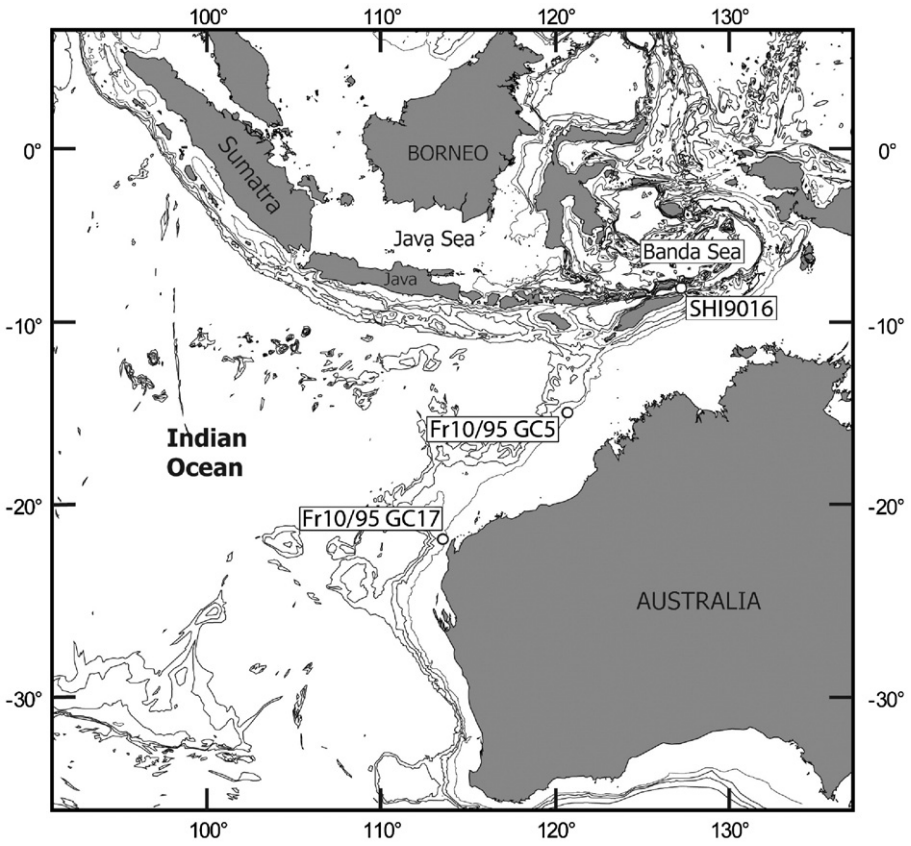

Fig. 1. Map showing the location of the selected cores from the eastern Indian Ocean.

In order to solve some of the conflicting views, we studied three cores collected from offshore Western Australia and from the Banda Sea, and in particular to investigate: (a) possible modifications in benthic foraminifera distribution due to climatic changes during the last 40 kyrs, in addition to intensity variations of the intermediate- and deep-water circulation; (b) the past position the Antarctic Intermediate Water and Indonesian Intermediate Water (AAIW–IIW); and (c) productivity levels of the Banda Sea and off the west coast of Western Australia during the LGM.

Table 1
List of the cores used in this study

Core	Type	Latitude S	Longitude E	Water depth (m)	Sampling interval (cm)	Previous work
Fr10/95 GC17	Gravity core	22°07.74′	113°30.11′	1093	4	Martinez et al. (1999) Takahashi and Okada, 2000 Gingele et al. (2001) van der Kaars and De Deckker (2002)
Fr10/95 GC5	Gravity core	14°00.55′	121°01.58′	2452	4	Olley et al., 2004 Martinez et al. (1999) Gingele et al. (2001) Maeda (2003)
SHI9016	Piston core	8°27.35′	127°53.83′	1802	4	Ahmad et al. (1995) Spooner et al. (2005) Gingele et al. (2001)

2. Materials and methods

2.1. Materials

Three cores were studied for detailed micropalaeontological analysis covering the last 30 kyrs with an extension up to 62 kyrs for one core. For location and core details see Fig. 1 and Table 1. Two gravity cores were recovered during the *RV Franklin* cruise, Fr10/95 in 1995 offshore Western Australia whereas a piston core (SHI9016) was collected during the SHIVA cruise in 1990 by the *RV Baruna Jaya* (see acknowledgements section). Cores selection was based on the information available regarding the oceanographic settings and the results obtained from analysis of Recent benthic foraminifera for the same region (Murgese and De Deckker, 2005).

Based in sediment colour, along core Fr10/95 GC17, two clay units are recognised (Fig. 2a): a yellowish brown clay unit (first 88 cm) separated by a transition interval (between 88 cm and 108 cm) from a second unit represented by a greyish-olive clay (from 108 cm to 178 cm). Below 80 cm, minor bioturbation is observed and, between 160 cm and 170 cm, non-parallel lamination is also present. Core Fr10/95 GC5 consists of greyish olive clay, with alternating laminations and minor bioturbation (Fig. 2b). The sediments of the section studied from SHI9016 consist predominantly of grey or olive-grey clay, with sandy levels at 160 cm and lamination between 50 cm and 60 cm (Fig. 2c).

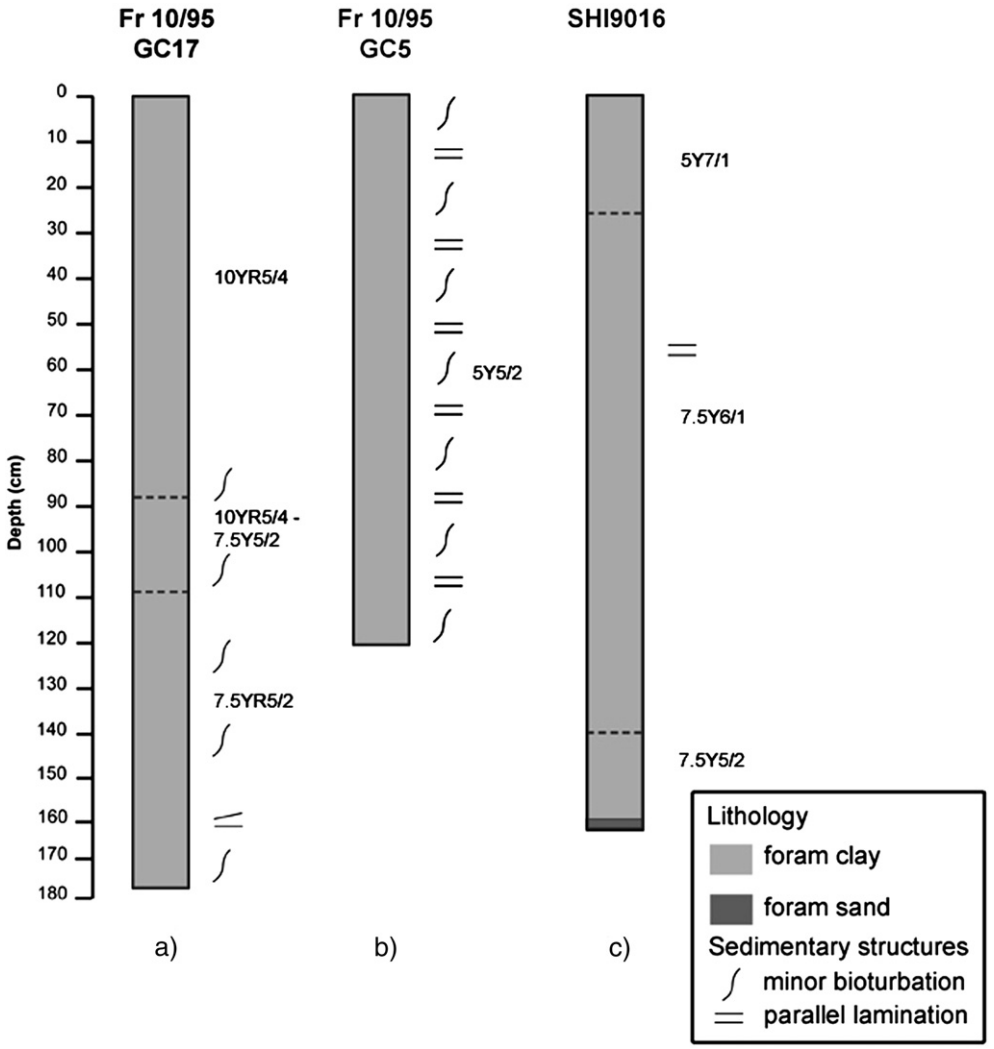

Fig. 2. Lithological logs of the studied cores: (a and b) Fr10/95 GC17 and GC 5 adapted from Martinez et al. (1999); (c) SHI9016 is adapted from Spooner et al. (2005). For more details refer to text.

2.2. Faunal analyses

The analysis of the benthic foraminiferal faunas from gravity cores Fr10/95 GC17 and Fr10/95 GC5 was completed for the same samples (3 cm^3 in volume) processed by Martinez et al. (1999) who studied the cores at 2 cm intervals. Samples were dried in an oven to obtain dry weight and then soaked in a dilute (3%) hydrogen peroxide solution until the clays had fully disaggregated. Samples were then washed with a gentle water jet through a 63 μm sieve and the coarse fraction dried at 40 °C. For piston core SHI9016, approximately 5–6 cm^3 of sediment were processed following the same procedure mentioned above, but sampling was at 5 cm intervals.

Benthic foraminifers from the >150 μm fraction of each sample were isolated, counted and mounted on micropalaeontological slides. The identification of benthic foraminifera was conducted on the basis of the descriptions in the Ellis and Messina catalogue (Ellis and Messina, 1940), and Barker (1960), Phleger et al. (1953), Corliss (1979), Van Marle (1988) and Hess (1998) publications. The absolute number of individuals for each species was converted as the percentage of total foraminifera present in each sample.

Species present with a percentage >2% in at least 1 sample were used for statistical analyses. The specimens belonging to the genera *Fissurina*, *Lagena*, *Lenticulina*, *Oolina* and *Parafissurina* were present in many samples with high species diversity, with each taxon displaying generally low percentages (<2.5%). For this reason, all the species belonging to these genera were used for statistical analysis but were grouped together as *Fissurina* spp., *Lagena* spp., *Lenticulina* spp., *Oolina* spp. and *Parafissurina* spp.

The program STATISTICA 5.0 was used to perform *Q*-mode Factor Analysis on the species data set of each core. The number of species >2% in at least one sample varied and the number of taxa included for statistical analyses for each core is listed in Table 2. Based on the percentages of species identified in the samples, the faunal diversity (expressed as the Fisher's Alpha index (α) (Williams, 1964), the Shannon-Weaver index *H*(*S*) (Murray, 1991), the equitability (*E*) (Murray, 1991), the dominance (*D*) (den Dulk, 2000)), the percentage of porcellaneous taxa and the percentage of presumed infaunal calcareous benthic foraminifera were calculated. The infaunal-calcareous species were those considered for studies in recent benthic foraminifera from the same region (Murgese and De Deckker, 2005).

Table 2
Number of benthic foraminifera species included for statistical analyses in each core and average number of specimens counted for each core

	Fr10/95 GC17	Fr10/95 GC5	SHI9016
No. of species	52	36	55
Average number of specimens counted	171	336	184

The total number of foraminifera isolated in each sample was used to calculate the benthic foraminifera accumulation rate (BFAR), following the formula proposed by Herguera and Berger (1991):

$$\mathrm{BFAR} = (F)\cdot(\mathrm{LSR})\cdot(\mathrm{DBS})[\mathrm{n/cm^2kyr}];$$

where *F* is the abundance of foraminifera (n/g), LSR is the linear sedimentation rate (cm/kyr) and DBS is the dry bulk sediment (g/cm^3) (g = grams of dry sediment).

The accumulation rate (AR) for the species (*Bulimina aculeata*, *Uvigerina proboscidea*, *Epistominella exigua*), quantitatively relevant in all cores, was also calculated applying Heguera and Berger's (1991) formula as follows:

$$\mathrm{AR} = (\mathrm{n/g})\cdot(\mathrm{LSR})\cdot(\mathrm{DBS})[\mathrm{n/cm^2kyr}];$$

where n/g indicates the abundance of species in the sample.

2.3. Age models

The age model for Fr10/95 GC17 was proposed by Martinez et al. (1999), who based it on the $\delta^{18}O$ record of *G. sacculifer* (without a sac-like final chamber). That model was supplemented later by 13 AMS ^{14}C dates (van der Kaars and De Deckker, 2002) and Olley et al. (2004) supplemented the dating with optically stimulated luminescence dates done on single quartz grains from the same core. The section studied here covers the last 30 kyr BP (Fig. 3a). The age model for Fr10/95 GC5 was proposed by Gingele et al. (2001), who used a combination of the $\delta^{18}O$ record of *G. sacculifer* (0–93 cm), as measured by Martinez et al. (1999), and the $\delta^{18}O$ record of *Globigerinoides ruber* (93–122 cm). Due to the different habitats characterising the two species, a value of 1‰ was subtracted from all the $\delta^{18}O$ values of *G. ruber* (Gingele et al., 2001). One AMS date is available for foraminifers taken at depth 57–58 cm, which has a calibrated age of 20.4 kyr BP (Gingele et al., 2001) and the base of the studied section was given an age of 35 kyr BP (Fig. 3b). The age model for piston core SHI9016 was originally proposed by Gingele et al. (2001) and further confirmed with 7 AMS dates provided by Spooner et al. (2005). Chronology of the core is based on the $\delta^{18}O$ record of *G. ruber* combined with the AMS dates from Spooner et al. (2005) and

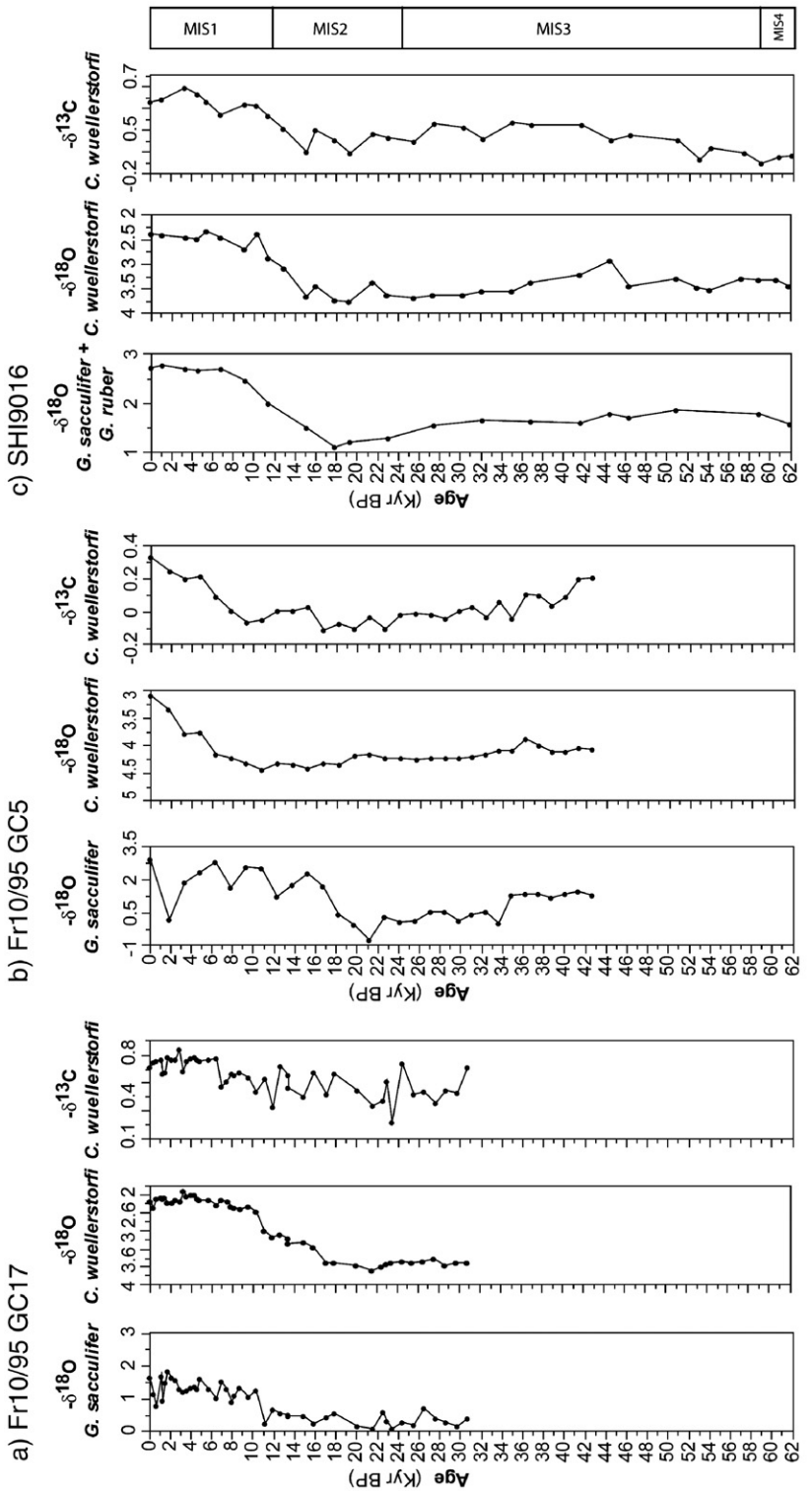

Fig. 3. Plot of the $\delta^{18}O$ and $\delta^{13}C$ data for the 3 studied cores from the eastern Indian Ocean.

the base of the studied section was given an age of 62 kyr BP (Fig. 3c).

The isotope records for the cores were calibrated against the SPECMAP chronology (Martinson et al., 1987) using the *Analyseries* software (Paillard et al., 1996). All ages presented here are in calibrated years BP.

2.4. $\delta^{18}O$ and $\delta^{13}C$ isotope analyses

The $\delta^{18}O$ and the $\delta^{13}C$ isotopic signals from *C. wuellerstorfi* (specimens handpicked from the >250 μm fraction) were measured in order to acquire information about the deep-water circulation and/or the presence of organic matter at the sea floor (Fig. 3a–c). A number of specimens sufficient to reach the minimum weight of material (180 μg) detectable by the mass spectrometer, were handpicked from each sample from the >250 μm fraction. Specimens were then washed in alcohol and placed in an ultrasonic cleaner for 10 s in order to eliminate any contaminating residual adhering to the foraminifer test. Oxygen- and carbon-isotopic data obtained are reported in the usual notation, which is referred to the PeeDee belemnite (V-PDB) standard. Samples were calibrated against the National Bureau of Standards calcite (NBS-19), assuming values of $\delta^{18}O_{V\text{-}PDB} = -2.20‰$ and $\delta^{13}C_{V\text{-}PDB} = -1.95‰$. For cores Fr10/95 GC5 and SHI9016, analyses were conducted utilising a Finnigan-MAT 251 mass spectrometer at the Research School of Earth Sciences (RSES) at the Australian National University (ANU). The external errors of stable isotopes were: ±0:05‰ PDB for $\delta^{18}O$ and ±0:08‰ PDB for $\delta^{13}C$. Isotope analyses of benthic foraminifera from gravity core Fr10/95 GC17 were processed in the same way using the Finnigan-MAT 251 mass spectrometer at the GEOMAR Institute in Kiel, Germany. The external errors of stable isotope analyses were: ±0:08‰ PDB for $\delta^{18}O$ and ±0:06‰ PDB for $\delta^{13}C$. *G. ruber* (150–250 μm size fraction). Specimens from the lower portion of core Fr10/95-GC5 were analysed for their isotopic composition using a Micromass OPTIMA at the Geological Survey of Japan where standard deviation for the $\delta^{18}O$ was ±0.11‰.

3. Results

3.1. Foraminiferal analyses

A total of 182 benthic foraminifera species were recognised in the samples collected from core Fr10/95 GC17 and a total of 87 benthic foraminifera

Table 3
Q-mode Factor Analysis (principal components) results for gravity core Fr 10/95 GC17

Species	F1	F2	F3	Species	F1	F2	F3
Astrononion echolsi	−0.43	−0.48	0.59	*Hoeglundina elegans*	−0.15	1.51	−0.35
Bolivina robusta	3.23	−0.72	0.11	*Karreriella bradyi*	−0.27	−0.04	−0.78
Bolivinita quadrilatera	−0.55	−0.49	0.01	*Lagena* spp.	−0.24	−0.30	−0.48
Brizalina dilatata	0.88	−1.08	0.22	*Lenticulina* spp.	−0.12	−0.64	−0.40
Bulimina aculeata	−0.53	0.63	−0.98	*Martinottiella communis*	−0.38	−0.59	−0.59
Bulimina alazanensis	−0.45	−0.72	−0.58	*Melonis barleeanum*	−0.08	−0.52	−0.21
Bulimina costata	−0.17	−0.33	−0.55	*Melonis pompilioides*	−0.61	−0.65	−0.25
Ceratobulimina pacifica	0.24	−0.35	1.07	*Miliolinella oblonga*	−0.36	−0.30	−0.27
Chilostomella oolina	−0.22	−0.43	−0.56	*Nummoloculina contraria*	−0.57	−0.41	−0.14
Cibicidoides bradyi	0.48	−0.04	2.10	*Nummoloculina irregularis*	0.58	1.40	3.04
Cibicidoides kullenbergi	−0.37	0.12	0.14	*Oridorsalis tener umbonatus*	0.07	−0.34	0.15
Cibicidoides pseudoungerianus	0.40	0.80	0.93	*Osangularia cultur*	0.20	−0.41	0.73
Cibicidoides robertsonianus	−0.42	−0.46	−0.36	*Pullenia bulloides*	−0.19	−0.09	−0.21
Cibicidoides wuellerstorfi	−0.16	4.21	0.18	*Pullenia quinqueloba*	−0.19	−0.49	−0.29
Dentalina inornata	−0.35	−0.66	−0.82	*Pyrgo elongata*	−0.32	−0.31	−0.21
Dorothia bradyana	−0.50	−0.04	−0.81	*Pyrgo murrhina*	−0.13	−0.13	0.07
Ehrenbergina trigona	0.01	3.08	−1.00	*Quinqueloculina seminulum*	0.18	0.57	0.12
Epistominella umbonifera	−0.27	−0.67	−0.40	*Robertina tasmanica*	−0.36	−0.39	−0.19
Fissurina spp.	−0.27	0.27	−0.43	*Sigmoilopsis schlumbergeri*	−0.40	−0.41	−0.06
Fursenkoina fusiformis	−0.35	−0.39	−0.45	*Sphaeroidina bulloides*	1.03	0.24	0.29
Gavelinopsis lobatulus	−0.06	−0.15	0.20	*Textularia lythostrota*	−0.52	−0.03	−0.80
Globocassidulina subglobosa	−0.49	−1.05	4.86	*Textularia pseudogramen*	−0.40	−0.10	−0.49
Gyroidinoides orbicularis	−0.09	−0.71	0.44	*Triloculina subvalvularis*	−0.30	−0.21	−0.39
Gyroidinoides polius	−0.37	−0.49	−0.82	*Triloculina tricarinata*	−0.19	−0.21	−0.11
Gyroidinoides soldanii	−0.07	−0.38	−0.04	*Uvigerina peregrina*	−0.60	2.95	0.50
Hauerinella incostans	−0.53	0.22	−0.63	*Uvigerina proboscidea*	5.72	0.15	−1.08

species were recognised in the samples collected from core Fr10/95 GC5. The analysis of benthic foraminifera species, extracted from samples from piston core SHI9016, led to the identification of 138 taxa.

In core Fr10/95 GC17, three varimax factors were calculated, accounting for 77% of the total variance of the species analysed. According to species scores (Table 3) and factor loadings (Fig. 4a), the following downcore faunal changes can be described: *C. wuellerstorfi*

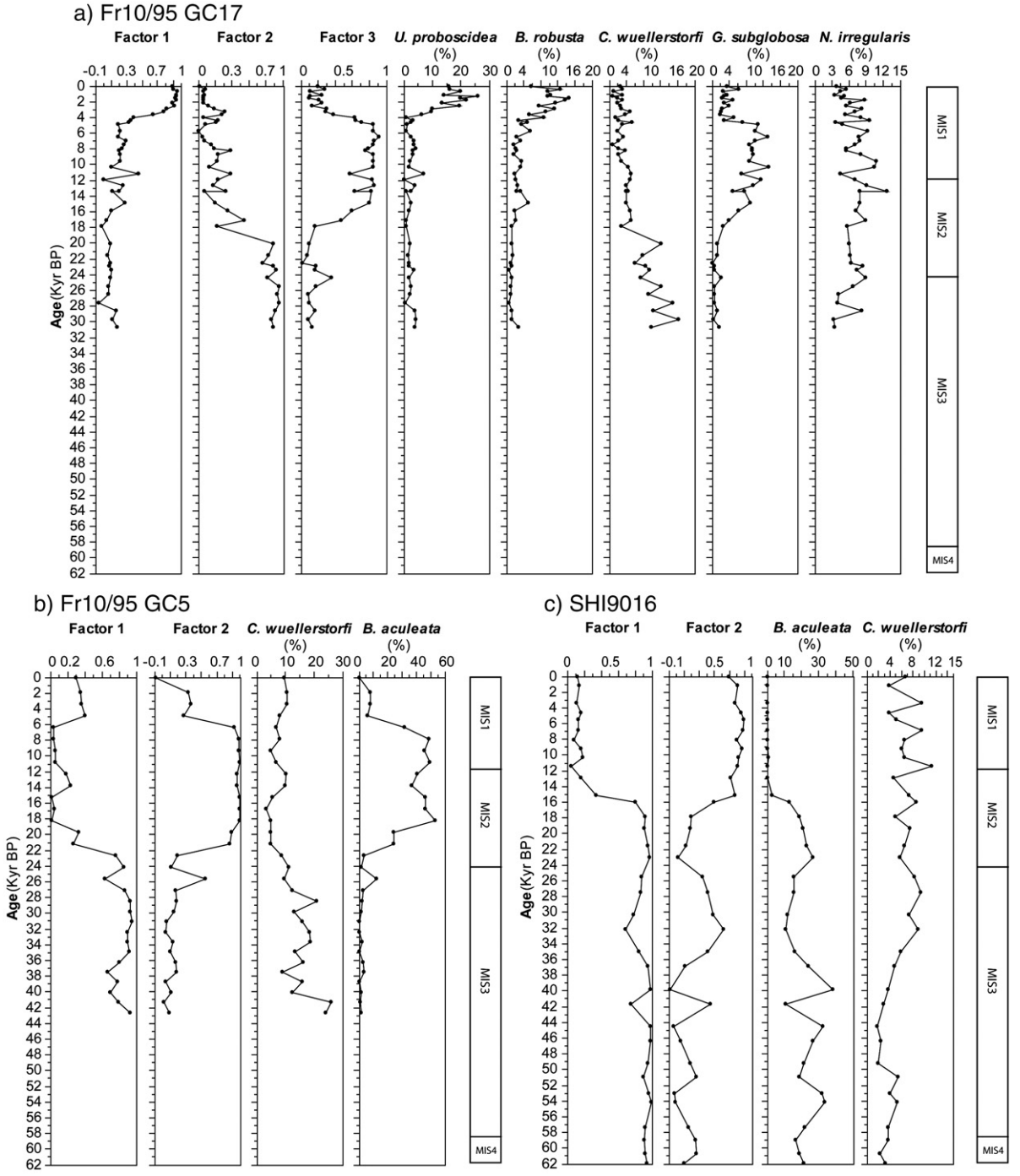

Fig. 4. *Q*-mode varimax factor loadings and dominant species percentages for the samples of the three studied cores plotted vs. age (cal. kyr BP).

assemblage (varimax factor F2) characterised the benthic foraminiferal fauna from 31 to 18 kyr BP (termination of MIS3-mid MIS2), *Globocassidulina subglobosa* and *Nummoloculina irregularis* assemblage (varimax factor F3) dominated between 17 and 4 kyr BP (mid MIS2-mid MIS1), and *Bolivina robusta* and *U. proboscidea* assemblage (varimax factor F1), that with the species *B. robusta*, dominated during the last 4 kyrs (late MIS1). Two varimax factors, explaining 80% of the total species variance, were calculated by *Q*-mode Factor Analysis (Principal Components) for core Fr10/95 GC5. The analysis of species scores (Table 4) and factor loadings (Fig. 4b) led to the identification of two assemblages that are dominated respectively by the species *C. wuellerstorfi* (varimax factor F1) and *B. aculeata* (varimax factor F2). These assemblages characterised the benthic foraminiferal fauna in core Fr10/95 GC5 during two distinct periods: *C. wuellerstorfi* dominated between 35 kyr BP and 18 kyr BP, and *B. aculeata* dominated the samples between 18 kyr BP and 4 kyr BP (Fig. 4b). For core SHI9016, factor analysis calculated two varimax factors, explaining 82.7% of the total variance of the species distribution. The species scores (Table 5) indicate two assemblages: one dominated by *B. aculeata* (varimax factor F1) and another dominated by *C. wuellerstorfi* (varimax factor F2). According to factor loadings (Fig. 4c), these assemblages characterised the samples from core SHI9016 related to two distinct periods: from 62 until 15 kyr BP, *B. aculeata* dominated the benthic foraminiferal fauna, while *C. wuellerstorfi* dominated during the last 15 kyrs.

Table 4
Q-mode Factor Analysis results for the reduced species data set of gravity core Fr10/95 GC5

Species	F1	F2	Species	F1	F2
Astrononion echolsi	0.91	−0.04	*Melonis pompilioides*	−0.10	−0.21
Bulimina aculeata	−1.06	5.67	*Oolina* spp.	−0.50	−0.23
Bulimina costata	−0.05	−0.18	*Oridorsalis tener umbonatus*	1.90	0.29
Cassidulina laevigata	0.07	−0.17	*Osangularia cultur*	−0.59	−0.33
Ceratobulimina pacifica	−0.77	−0.32	*Parafissurina* spp.	−0.21	−0.21
Chilostomella oolina	2.12	0.71	*Pullenia bulloides*	−0.42	−0.28
Cibicidoides bradyi	−0.81	−0.27	*Pullenia quinqueloba*	−0.55	−0.17
Cibicidoides robertsonianus	−0.62	−0.33	*Pyrgo depressa*	−0.62	−0.29
Cibicidoides wuellerstorfi	3.49	0.09	*Pyrgo murrhina*	1.58	−0.11
Epistominella exigua	1.59	0.58	*Pyrgo* sp.	−0.28	−0.30
Fissurina spp.	0.41	−0.20	*Quinqueloculina seminulum*	−0.34	−0.26
Globobulimina affinis	−0.32	−0.24	*Quinqueloculina venusta*	−0.64	−0.25
Globobulimina pacifica	−0.56	−0.27	*Robertinoides bradyi*	−0.68	−0.30
Globocassidulina subglobosa	−0.53	−0.22	*Sigmoilopsis schlumbergeri*	−0.42	−0.28
Gyroidinoides orbicularis	−0.33	−0.23	*Sphaeroidina bulloides*	−0.60	−0.20
Hoeglundina elegans	−0.11	−0.29	*Uvigerina peregrina*	1.02	−0.13
Lagena spp.	−0.49	−0.27	*Uvigerina porrecta*	−0.59	−0.33
Laticarinina pauperata	−0.56	−0.29	*Uvigerina proboscidea*	−0.34	−0.12

3.2. Faunal characteristics

For each sample, the following parameters, which provide faunal characteristics, were calculated: the percentage of porcellaneous taxa, the percentage of infaunal taxa, Fisher's Alpha index (α), Shannon-Weaver index ($H(S)$), equitability (E) and dominance (D).

Porcellaneous and infaunal species percentages for core Fr 10/95 GC17 are shown in Fig. 5a. Porcellaneous taxa displayed the highest percentages between 24 and 8 kyr BP (MIS2-early MIS1) while, before and after this period, the group was generally less frequent (Fig. 5a). Infaunal taxa percentages increased from 31 to 17 kyr BP. Between 17 and 4 kyr BP, this group displayed values always <30%. High percentages (about 30%) are recorded for infaunal species throughout the studied section. The highest percentages are recorded for samples related to the last 4 kyrs. Diversity index curves follow similar patterns (Fig. 5a). The α, $H(S)$ and E indexes were characterised by high values until 4 kyr BP. Reduced species diversity is recorded from that timing until today (late MIS1). Dominance followed an opposite trend (Fig. 5a), showing the highest values for the period which covers the last 4 kyrs. In core Fr 10/95 GC5, porcellaneous taxa percentages, from 35 to 22 kyr BP (termination of MIS3 to early MIS2), ranged between 15% and 20%, with a peak at the beginning of MIS2 (Fig. 5b). From this point until the Present, the percentage of this group of species always remained below 15%. Infaunal species, from 35 to 18 kyr BP (termination of MIS3 to mid MIS2), showed percentages <50%. Between 18 and 5 kyr BP (termination of MIS2 to mid MIS1), the percentages were high (>60%). They decreased towards the Present, taking on values

Table 5
Q-mode Factors Analysis results for the reduced species data set of piston core SHI9016

Species	F1	F2	Species	F1	F2
Anomalina globulosa	−0.30	−0.50	*Karreriella bradyi*	−0.34	−0.71
Astrononion echolsi	0.36	0.54	*Lagena* spp.	0.05	−0.15
Bolivina robusta	−0.39	−0.43	*Laticarinina pauperata*	−0.35	−0.38
Bulimina aculeata	6.61	−2.02	*Lenticulina spp.*	−0.39	−0.33
Bulimina costata	−0.34	0.11	*Martinottiella communis*	−0.33	−0.51
Buliminella elegantissima	−0.37	−0.66	*Melonis barleeanum*	0.64	−0.27
Cassidulina crassa	−0.34	−0.68	*Melonis pompilioides*	−0.17	−0.76
Cassidulina laevigata	0.25	0.25	*Nummoloculina irregularis*	−0.38	−0.39
Ceratobulimina pacifica	−0.52	0.27	*Oolina* spp.	−0.37	−0.55
Chilostomella oolina	−0.53	1.17	*Oridorsalis tener umbonatus*	0.66	1.22
Cibicidoides bradyi	0.80	0.80	*Parafissurina spp.*	−0.24	0.02
Cibicidoides kullenbergi	−0.48	−0.17	*Pullenia bulloides*	0.30	2.71
Cibicidoides pseudoungerianus	−0.46	0.44	*Pullenia quinqueloba*	0.09	0.25
Cibicidoides robertsonianus	−0.34	−0.62	*Pyrgo depressa*	−0.15	0.08
Cibicidoides wuellerstorfi	0.48	2.90	*Pyrgo murrhina*	−0.04	−0.07
Cibicidoides sp.	−0.30	−0.65	*Pyrulina gutta*	−0.41	−0.68
Dentalina communis	−0.40	−0.52	*Quinqueloculina lamarckiana*	−0.41	−0.54
Eggerella bradyi	−0.33	−0.50	*Quinqueloculina seminulum*	−0.27	0.13
Ehrenbergina trigona	−0.11	−0.52	*Quinqueloculina venusta*	−0.28	−0.71
Epistominella exigua	0.62	−0.79	*Robertina tasmanica*	−0.40	−0.70
Fissurina spp.	0.91	2.03	*Robertinoides brady*	−0.41	−0.73
Gavelinopsis lobatulus	−0.16	−0.41	*Sigmoilopsis schlumbergeri*	−0.23	−0.24
Globocassidulina elegans	−0.49	−0.27	*Siphotextularia* sp.	−0.41	−0.67
Globocassidulina subglobosa	0.08	2.70	*Sphaeroidina bulloides*	−0.42	−0.15
Gyroidinoides altiformis	−0.34	−0.50	*Triloculina tricarinata*	−0.21	−0.30
Gyroidinoides orbicularis	−0.15	0.35	*Uvigerina proboscidea*	1.47	2.79
Gyroidinoides soldanii	−0.29	−0.50	*Valvulineria araucana*	−0.16	−0.88
Hoeglundina elegans	−0.32	0.71			

similar to those seen for the older part of the studied section of the core, being again <50% (Fig. 5b). Diversity indices followed similar patterns (Fig. 5b): the α, *H*(*S*) and *E* indices were characterised by low values, especially between 18 and 5 kyr BP (termination of MIS2 to mid MIS1), while, for the last 5 kyrs (late MIS1), they indicated increased species diversity. An opposite trend was shown by dominance (Fig. 5b), which reached the highest values between the end of MIS2 and the mid MIS1, while from 35 to 18 kyr BP and for the last 5 kyrs, this parameter showed lower values (<20%). In core SHI9016, porcellaneous species showed low percentages for the studied time interval (Fig. 5c). The infaunal taxa followed two major patterns. Before 15 kyr BP (termination of MIS4-mid MIS2), they were characterised by percentages >75%, but these were lower (generally <75%) for the last 15 kyrs (termination of MIS2 to MIS1). During this period, the percentages showed an irregular pattern, ranging between 64% and 77%. Diversity indices (α, *H*(*S*), and *E*) calculated for the SHI9016 samples displayed similar trends, whereas Dominance was characterised by an inverse pattern (Fig. 5c). Before 16 kyr BP (termination of MIS4 to mid-MIS2), faunal diversity was characterised by low values, while, during the last 16 kyrs (termination of MIS2 to MIS1), it increased, by maintaining higher values compared to the former time interval and showing high values (>15%). Dominance showed higher values during the period comprised between termination of MIS4 and early to mid-MIS2 (62 kyr BP-16 kyr BP), compared to those recorded for last 16 kyrs.

3.3. Benthic foraminifera accumulation rate (BFAR) and accumulation rates calculated for B. aculeata, E. exigua and U. proboscidea

Benthic foraminifera accumulation rate (BFAR), calculated for core Fr10/95 GC17 samples, ranged between 600 and 800 n/cm^2/kyr (n=number of benthic foraminifera), from 32 to 15 kyr BP (termination of MIS3 to termination of MIS2), following a rather regular pattern (Fig. 6a). At 13 kyr BP, the BFAR decreased down to a value of 301 n/cm^2/kyr. This minimum was followed by a sudden increase, with a peak of 922 n/cm^2/kyr, at 10 kyr BP. The BFAR decreased again during the following 5 kyrs, reaching another minimum value at 5 kyr BP (317 n/cm^2/kyr).

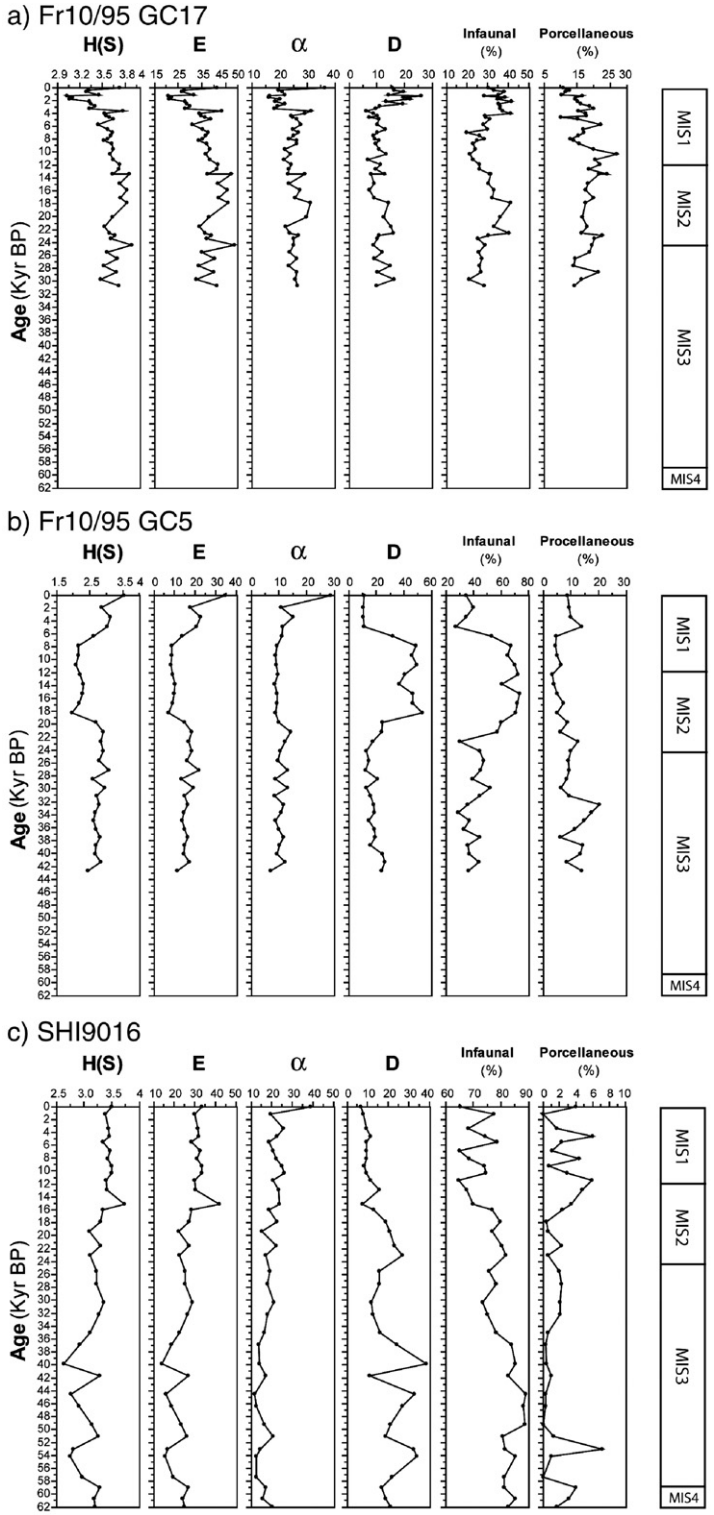

Fig. 5. Faunal characteristics (species diversity indexes ($H(S)$, E, α, dominance (D))), faunal and porcellaneous species percentages) down-core variations for the three studied cores plotted vs. age (cal. kyr BP).

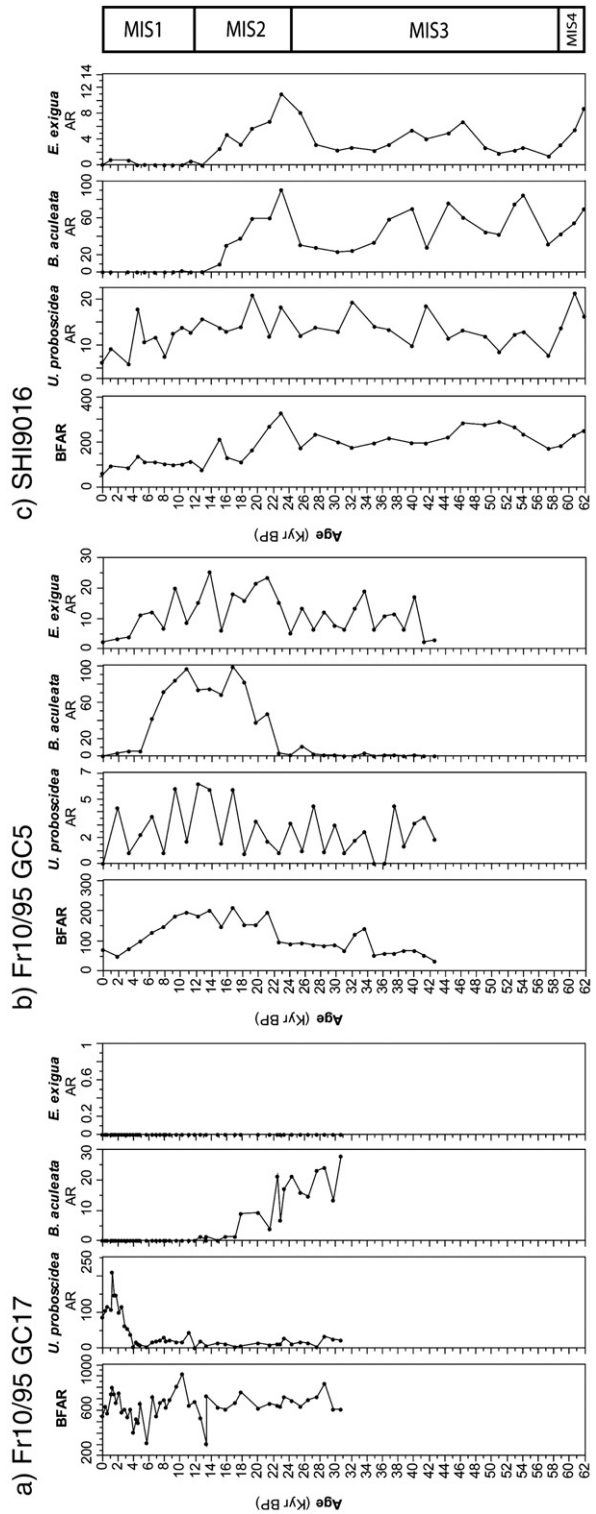

Fig. 6. Benthic Foraminiferal Accumulation Rate (BFAR), plus *U. proboscidea*, *B. aculeata* and *E. exigua* accumulation rates calculated for the samples from the three cores samples and plotted vs. age (cal. kyr BP).

During the last 5 kyrs, the BFAR increased until 1 kyr BP, reaching 799 n/cm^2/kyr and then decreased to 547 n/cm^2/kyr for the Present. The accumulation rate (AR) calculated for the species *B. aculeata*, *E. exigua* and *U. proboscidea* is plotted in Fig. 6a. *E. exigua* was never found in the benthic foraminiferal assemblage at this core site. *B. aculeata* displayed generally very low values during the last 30 kyrs, with an accumulation rate of ~20 n/cm^2/kyr recorded before the LGM. The *U. proboscidea* AR remained below 50 n/cm^2/kyr between 30 kyr BP and 4 kyr BP. During the last 4 kyrs, the *U. proboscidea* AR increased by reaching a maximum value of 210 n/cm^2/kyr at 1 kyr BP.

The accumulation rate of benthic foraminifera, for the last 42 kyrs, at the Fr10/95 GC5 site is displayed in Fig. 6b. Between 42 and 20 kyr BP, the BFAR increased, passing from 70 to 92 n/cm^2/kyr. At 24 kyr BP, the BFAR reached values close to 140 n/cm^2/kyr. Between 20 and 5 kyr BP, the BFAR was characterised by high values, which ranged between 150 and 200 n/cm^2/kyr. During the last 5 kyrs, the BFAR decreased, passing from 200 to 70 n/cm^2/kyr. The accumulation rates (AR) calculated for *B. aculeata*, *E. exigua* and *U. proboscidea* are shown in Fig. 6b. When the *B. aculeata* AR reached values of 45 n/cm^2/kyr, at the LGM, *E. exigua* passed from 15 to more than 20 n/cm^2/kyr. Between 20 and 5 kyr BP, these two species were characterised by an AR ranging between 40 and 100 n/cm^2/kyr, and between 5 and 25 n/cm^2/kyr, respectively. *U. proboscidea*, despite never reaching high AR during the last 30 kyrs, displayed values close to 5 n/cm^2/kyr soon after the LGM and this pertained until today.

For the core SHI9016 samples, the curve related to the BFAR (Fig. 6c) displays two major patterns. Between 62 and 20 kyr BP, the BFAR was characterised by high values (=200 n/cm^2/kyr) with a peak of 326 n/cm^2/kyr, at 23 kyr BP. After 15 kyr BP, the benthic foraminifera AR decreased, maintaining values close to 100 n/cm^2/kyr, which decreased to 50 n/cm^2/kyr for the Present. The *B. aculeata* AR mirrored the BFAR trend (Fig. 6c). Between 62 and 15 kyr BP, *B. aculeata* AR ranged between 20 and 90 n/cm^2/kyr. After 15 kyr BP, this species was absent at this site. *E. exigua* showed a similar pattern, with AR ranging between 5 and 20 n/cm^{2}kyr, before 15 kyr BP, and disappearing after that period. *U. proboscidea* was still present after 15 kyr BP, but as for the other two species, it displayed higher AR values (>10 n/cm^2/kyr) between 62 and 15 kyr BP. During the last 15 kyrs, the *U. proboscidea* AR decreased constantly from 10 to 5 n/cm^2/kyr until today.

3.4. ^{13}C results

$\delta^{13}C$ values obtained from the test composition of *C. wuellerstorfi* specimens, collected from the three cores, are shown in Fig. 3a–c. The values obtained with the $\delta^{13}C$ analysis of *C. wuellerstorfi* from Fr10/95 GC17 range between 0.74‰ and 0.22‰. The maximum value (0.74‰) is referred to 3 kyr BP and the minimum (0.22‰) to 23 kyr BP. The analysis related to the time interval between 31 kyr BP and 7 kyr BP gave values, which ranged between 0.22‰ and 0.64‰. Isotopic values obtained for the last 7 kyrs are all >0.5‰.

The $\delta^{13}C$ values from Fr10/95 GC5 range between 0.33‰ and −0.11‰. The minimum value (−0.11‰) is recorded at 11 kyr BP, while the maximum value (0.33‰) relates to the Present. The trend shown by $\delta^{13}C$ appears 'regular' with values constantly decreasing from 0.21‰ (35 kyr BP), to 0.03‰ (11 kyr BP), and then constantly increasing during the last 11 kyrs, reaching a value of 0.33‰ for the Present.

The $\delta^{13}C$ values from SHI9016 range between 0.59‰ and −0.1‰. The maximum value (0.59‰) is recorded at 3 kyr BP and the minimum (−0.10‰) at 59 kyr BP. The isotopic data follow a pattern characterised by the presence of two points where the values reach two minima. After a slight decrease, between 62 and 59 kyr BP, when $\delta^{13}C$ passed from −0.03‰ to −0.10‰, $\delta^{13}C$ increased, reaching 0.27‰ at 35 kyr BP. The $\delta^{13}C$ then shows a new relative minimum (−0.01‰) at 19 kyr BP and then constantly increases until the Present.

4. Discussion

4.1. Isotope analyses

Past variations at global scale of deep water $\delta^{13}C$ values emerged from the analysis of deep-sea cores collected from the three major oceans, with the $\delta^{13}C$ generally lower at the LGM, compared to the Holocene record (Duplessy et al., 1984; Curry et al., 1988; Sarnthein et al., 1988). This phenomenon is attributed to the reduction of the continental biosphere and the consequent transfer of organic carbon depleted in ^{13}C to the oceans (Adams et al., 1990; Shackelton, 1977). Calculations made on the data obtained from cores collected worldwide in the oceans suggest a $\delta^{13}C$ value of 0.46‰ more negative during the LGM (Curry et al., 1988). This value represents the mean of the differences between the interglacial $\delta^{13}C$ and glacial $\delta^{13}C$ (I–G $\delta^{13}C$), calculated for the four ocean basins. When these basins are considered separately the difference varies

from ocean to ocean (Curry et al., 1988). In the eastern Indian Ocean, the I–G $\delta^{13}C$ difference reported by Duplessy et al. (1989) is 0.32‰. Also, the I–G $\delta^{13}C$ differences recorded for the eastern Indian Ocean range between −0.29‰ (offshore South Australia) and 0.7‰ (Bay of Bengal); the difference between these two data is related to the depth of the cores. For cores collected at intermediate depths, the I–G $\delta^{13}C$ difference is on average smaller (0.23‰) than 0.32‰, while, for deep waters, the I–G $\delta^{13}C$ difference is larger (0.37‰) (Sarnthein et al., 1988; Naqvi et al., 1994; Ahmad et al., 1995; McCorkle et al., 1998). Duplessy et al. (1989) explained this phenomenon by suggesting that a strengthened intermediate water circulation and a more sluggish deep-water circulation determined this gradient at 2000 m depth. A gradient between intermediate- and deep-water masses during the LGM for the Indian Ocean was already proposed by Kallel et al. (1988). A similar result is reported for the Pacific Ocean (Herguera et al., 1992), suggesting that this situation could have been common for both the Indian and Pacific basins (Wells et al., 1994).

The $\delta^{13}C$ depletion measured for the LGM at the Fr10/95 GC17 site (0.17‰) is well above the average $\delta^{13}C$ depletion calculated for the Indian Ocean. This would suggest a more intense circulation at intermediate depths. The I–G $\delta^{13}C$ difference recorded for Fr10/95 GC5 (0.29‰) is lower than 0.32‰, indicating a reduced deep-water circulation during the LGM at that site. A $\delta^{13}C$ depletion, between 0.31‰ and 0.35‰, characterised the period between 10 and 5 kyr BP. Assuming a more active deep-water circulation after the LGM (Duplessy et al., 1984), this isotopic signal appears to be related to an increased amount of organic matter to the sea floor. Values measured for the LGM for SHI9016 range between 0.3‰ and 0.4‰. and are similar or lower than the $\delta^{13}C$ Indian Ocean's average depletion. Considering that this core was collected at a depth of 1802 m, a smaller depletion than or similar to 0.32‰ would be expected. This could indicate conditions of reduced circulation (Gingele et al., 2001) paralleled by an increased amount of organic matter supplied at this site.

4.2. Benthic foraminifera assemblages

The analysis of benthic foraminifera collected from the studied cores permitted the identification of four major assemblages that dominated the benthic foraminiferal fauna over the last 30 kyrs spanning back to 60 kyrs in one core. These are the *B. aculeata* assemblage, the *C. wuellerstorfi* assemblage, the *G. subglobosa–N. irregularis* assemblage and the *U. proboscidea–B. robusta* assemblage.

The *B. aculeata* assemblage dominated the benthic foraminiferal fauna in core Fr10/95 GC5 (between 22 and 6 kyr BP) and in core SHI9016 (between 62 and 14 kyr BP) (Fig. 4b–c). The appearance of *B. aculeata* coincided with an increase of the *U. proboscidea* and *E. exigua* accumulation rate (Fig. 6b–c). Today, in the eastern Indian Ocean, the presence of *E. exigua* is related to a periodic delivery (seasonal) of organic matter to the sea floor, whereas *U. proboscidea* is associated to high carbon flux rate due to higher primary productivity levels at the sea surface, and low oxygen levels due to the organic matter oxidation and the presence of oxygen-depleted Indian Intermediate (IIW) and North Indian Intermediate Waters (NIIW) (Murgese and De Deckker, 2005). These two taxa maintained high AR values for the periods during which *B. aculeata* displayed high percentages, suggesting that the presence of this latter species coincided with conditions of increased organic matter supply. This observation is also supported by high BFAR values (Fig. 6b–c), suggesting conditions of enhanced export of organic matter to the sea floor (Herguera and Berger, 1991). Analyses on recent and living (stained) benthic foraminifera show a relationship between the abundance of *B. aculeata*, the sediment organic carbon content (Collins, 1989; Mackensen et al., 1993; Miao and Thunell, 1993; Rathburn and Corliss, 1994) and shallow oxygen penetration within the sediment (Miao and Thunell, 1996). The distribution of *B. aculeata* also correlates with a high organic-carbon flux (>2 gC/m^2/year) in the Atlantic and Southern Oceans (Altenbach et al., 1999). For core Fr10/95 GC5, the increase in C_{org} MAR (Maeda, 2003) is paralleled by the dominance of *B. aculeata*. The organic matter oxidation would then have induced oxygen depletion at the sea floor and in the sediment pore-water, thus creating ideal conditions for *B. aculeata* to thrive. The faunal characteristics calculated for the samples dominated by this species indicate low diversity and high dominance (Fig. 5b–c), pointing towards low-oxygen conditions (Lutze and Coulbourn, 1983; Denne and Sen Gupta, 1991; Sen Gupta and Machain-Castillo, 1993; Jannink et al., 1998; den Dulk, 2000).

The *C. wuellerstorfi* assemblage dominates the benthic foraminiferal fauna between 32 and 18 kyr BP in core Fr10/95 GC17 (Fig. 4a), between 42 and 22 kyr BP in core Fr10/95 GC5 (Fig. 4b) and between 18 kyr BP to the Present in core SHI9016 (Fig. 4c). Today, in the eastern Indian Ocean, *C. wuellerstorfi* is typical of an environment characterised by a high dissolved-

oxygen concentration and a low carbon-flux rate (Murgese, 2003). Studies of living (rose-Bengal stained) specimens support this interpretation: *C. wuellerstorfi* is a species typical of environments characterised by low carbon-flux rate (Mackensen et al., 1985; Altenbach, 1992; Burke et al., 1993; Altenbach et al., 1999) or by pulsed fluxes of organic matter (Mackensen et al., 1985). Periods dominated by this taxon are characterised by high species-diversity, an increased percentage of porcellaneous species and a low infaunal-species relative abundance, indicating high oxygen levels and reduced organic matter supply (Murgese and De Deckker, 2005).

The *G. subglobosa–N. irregularis* assemblage dominated the benthic foraminiferal fauna for core FR10/95 GC17 between 18 and 4 kyr BP (Fig. 4a). Today, the distribution of *N. irregularis* is correlated with low productivity levels at the sea surface, high dissolved-oxygen concentrations and with the distribution of AAIW (Murgese and De Deckker, 2005), whereas *G. subglobosa* is typical of an environment characterised by a low carbon flux-rate and high dissolved-oxygen concentrations (Murgese, 2003 and references therein). Increased oxygen levels for the period when these species dominated are also suggested by the reduced *C. wuellerstorfi* $\delta^{13}C$ depletion compared to the mean isotopic composition of the total dissolved CO_2 in the eastern Indian Ocean, as the result of an enhanced ventilation of the intermediate water masses during the LGM (Duplessy et al., 1989). Furthermore, increased oxygen levels are also pointed out by the increased porcellaneous taxa percentage (Fig. 5a). The *U. proboscidea–B. robusta* assemblage, characterised the benthic foraminiferal fauna for core FR10/95 GC17 during the last 4 kyrs (Fig. 4a), indicates reduced oxygen levels and/or increased carbon-flux rate. As discussed earlier, *U. proboscidea* is associated to low-oxygen conditions and high carbon-flux rate. The distribution of *B. robusta* is limited to intermediate depths (700–2000 m) and to environments with low dissolved-oxygen concentrations (Murgese, 2003). A relationship between this taxon and low-oxygen levels was already ascribed for the Australian–Irian Jaya continental margin by Van Marle (1988).

4.3. Eastern Indian Ocean palaeoceanographic evolution

4.3.1. The Banda Sea

The dominance of *B. aculeata* assemblage, between 62 and 15 kyr BP, indicates increased productivity levels at the sea-surface and/or reduced oxygenation for the Banda Sea. During that period, the situation in the Banda Sea was quite different from today, with more arid conditions causing a reduction in rainfall (Barmawidjaja et al., 1993; van der Kaars and Dam, 1995) with excess of evaporation over precipitation engendering conditions of higher sea-surface salinity (Martinez et al., 1997, 1998b; De Deckker et al., 2002; van der Kaars and De Deckker, 2002). Under that scenario, the absence of a low-salinity cap (the Barrier Layer) allowed a shoaling of the thermocline, with a consequent extension of the Deep Chlorophyll Maximum (DCM) in shallower waters, thus enhancing primary productivity (Barmawidjaja et al., 1993; Spooner et al., 2005). This change was paralleled by increased *N. dutertrei* percentages (Barmawidjaja et al., 1993; Spooner et al., 2005). The flux of organic matter to the sea floor and its oxidation would have led to oxygen depletion at the sea floor, although a different cause for a reduced oxygenation could have been a reduced deep-water circulation, as the interpretation of the *C. wuellerstorfi* $\delta^{13}C$ signal in the eastern Indian Ocean would indicate. It is likely that the increased input of organic matter in an already poorly ventilated environment engendered favourable conditions for *B. aculeata*. This taxon was replaced by the suspension feeder species *C. wuellerstorfi* at 15 kyr BP. The high percentage of this species during the last 15 kyrs (Fig. 4c) indicates a reduced flux of organic matter to the sea floor, accompanied by a strengthening of the bottom currents. The absence of *E. exigua* indicates a reduced amount of organic matter at the sea floor and the constant decrease of the *U. proboscidea* AR indicates a low carbon-flux rate and increased ventilation (Fig. 6c) with the calculated BFAR for this period shows values 2–3 times lower than those recorded for the previous 45 kyrs (Fig. 6c). This change coincides with the onset of the last deglaciation and the climatic shift towards conditions similar to modern ones (van der Kaars and Dam, 1997). Coinciding with this climatic change, sea level rose, submerging the Indonesian platforms (Chappell et al., 1996) and precipitation increased (Martinez et al., 1997, 1998b; De Deckker et al., 2002; van der Kaars and De Deckker, 2002; van der Kaars et al., 2006). Under these conditions, the formation of a low-salinity cap, due to the excess of rainfall over evaporation, caused the deepening of the DCM and the consequent reduction of productivity at the sea surface (Barmawidjaja et al., 1993; Spooner et al., 2005). The presence of more intense bottom currents is indicated not only by the lower *U. proboscidea* AR,

but also by higher silt sedimentation relative to clay (Gingele et al., 2001).

4.3.2. Offshore northern Western Australia

The late MIS3 and early MIS2 are characterised by the dominance of *C. wuellerstorfi* assemblage. The *C. wuellerstorfi* $\delta^{13}C$ curve (Fig. 3b) displays values consistently higher than those recorded for the LGM. The percentage of *N. dutertrei* shows values similar to those recorded for the Late Holocene (Martinez et al., 1999) and the same is valid for the BFAR (Fig. 6b). These data substantiate oligotrophic condition at the sea floor and increased ventilation. At 18 kyr BP, the replacement of the *C. wuellerstorfi* assemblage by the *B. aculeata* assemblage (Fig. 4a), indicates increased productivity at the sea-surface and/or reduced oxygen levels at the sea-floor. The mass accumulation rate of organic carbon measured for core Fr10/95-GC5 (Maeda, 2003) was higher at the LGM compared to late MIS3 to early MIS2, further supporting the idea of increased productivity at the sea surface. The low $\delta^{13}C$ of *C. wuellerstorfi* during the LGM can also be associated with a reduced deep-water circulation, which in turn could have engendered low-oxygen conditions. From the data obtained from Fr10/95 GC5 a less ventilated environment ($\delta^{13}C$ of *C. wuellerstorfi*) is postulated with an ensuing increased amount of organic matter (*E. exigua* AR and BFAR) reaching the sea floor creating favourable conditions for the *B. aculeata* assemblage to thrive. After the LGM, the persistent low values of $\delta^{13}C$ of *C. wuellerstorfi* (Fig. 3b), the high percentage of *B. aculeata* (Fig. 4b), the high values of *E. exigua* AR and the BFAR (Fig. 6b) are the consequences of another process. From 14 kyr BP until 5 kyr BP, this region was characterised by substantial summer rains (Veeh et al., 2000; van der Kaars and De Deckker, 2002; van der Kaars et al., 2006). The consequent increased fluvial discharge, with more nutrients injected into the sea, would have favoured phytoplankton blooms. This hypothesis is further supported by the values measured for the mass accumulation rate of the organic carbon (Maeda, 2003). For the last 5 kyrs, the benthic foraminiferal fauna was characterised by high diversity (Fig. 5b) and no particular taxon seemed to dominate the assemblage. The BFAR values were lower than those recorded between 35 and 18 kyr BP (Fig. 6b). The high value displayed by the $\delta^{13}C$ of *C. wuellerstorfi*, the low percentage of *N. dutertrei* (Martinez et al., 1999) and the low mass-accumulation-rate of organic carbon (Maeda, 2003), suggest reduced carbon-flux to the sea floor; this being the lowest recorded value for the last 35 kyrs.

4.3.3. Offshore the west coast of Western Australia

The high percentages of *C. wuellerstorfi* between 31 and 18 kyr BP suggest oligotrophic conditions and increased ventilation at the sea floor, where sporadic amounts of organic matter were laterally advected by active bottom currents. Today, the presence of a low-salinity and less dense water, represented by the poleward-flowing Leeuwin Current offshore Western Australia, causes a deepening of the nutricline, thus preventing the production of organic matter and determining conditions of low productivity at the sea surface. During MIS3, a different pattern for the Leeuwin Current was suggested by Gingele et al. (2001), who indicate the absence/reduction of this current at this site. The presence of a shallower nutricline, during MIS3 to the early MIS2, was already suggested by studies on calcareous nannofossils (Takahashi and Okada, 2000). The $\delta^{13}C$ of *C. wuellerstorfi*, between 31 and 18 kyr BP, displays the lowest values recorded for the entire section, being 0.22‰ lower than the modern-day values (Fig. 3a). This value does not indicate a significant increase of the amount of organic matter at the sea floor. Furthermore, the BFAR and low accumulation rates of *U. proboscidea* and *B. aculeata* indicate oligotrophic conditions (Fig. 5a). The low relative percentage of infaunal species recorded for this period (Fig. 5a) infers an environment more suitable for epifaunal suspension feeder species. This implies a more active circulation at intermediate depths towards the end of MIS3 and the early phase of MIS2. The *C. wuellerstorfi* assemblage was replaced by *N. irregularis–G. subglobosa* assemblage, with the onset of the LGM (Fig. 4a). High percentages of *N. irregularis* between 17 and 4 kyr BP indicate an increased influence at this latitude by the AAIW over the scarcely oxygenated IIW and low productivity at the sea surface.

The *C. wuellerstorfi* $\delta^{13}C$ values for this period are higher compared to those recorded before 20 kyr BP. The $\delta^{13}C$ depletion recorded for the LGM at this site is 0.19‰, smaller than the average depletion of 0.32‰ calculated for the Indian Ocean. The minor variation compared to the global signal was explained by Duplessy et al. (1989) as the result of an enhanced ventilation of the intermediate water masses during the LGM. High dissolved-oxygen concentrations at intermediate depths and low productivity at the sea surface were maintained until 4 kyr BP, when the assemblage dominated by *N. irregularis* and *G. subglobosa* was replaced by one dominated by *U. proboscidea* and *B. robusta* (Fig. 4a); this indicates low oxygen levels and increased carbon-flux rate. During the last 5 kyrs, the Leeuwin Current increased its strength (De Deckker,

2001; van der Kaars and De Deckker, 2002); the presence of a low-salinity cap, typical of the Leeuwin Current, could have also engendered a more stratified water column. Similar to what happened at the sea surface, the influence of the Indonesian waters at intermediate depths, with the IIW becoming more important, could explain a reduction of dissolved-oxygen concentrations. The high percentage of *U. proboscidea* and *B. robusta* implies this scenario. This is further corroborated by the faunal characteristics (low diversity (α, $H(S)$, E) and high dominance (D)) of the benthic foraminiferal assemblage during the last 5 kyrs (Fig. 5a). Nevertheless, the $\delta^{13}C$ of *C. wuellerstorfi* recorded over the last 5 kyrs (with the highest values measured) does not confirm this hypothesis. The BFAR for this time interval gives values similar to those recorded for the former 25 kyr and does not indicate any productivity increase (Fig. 5a). The increased percentages of *U. proboscidea* and infaunal taxa also suggest increased carbon-flux rate. In this case, in the presence of low dissolved-oxygen levels, the oxidation of organic matter would have been slower. Our interpretation is that the "food" availability at the sea floor increased, even with no variation of primary productivity at the sea surface.

5. Conclusions

The study of benthic foraminifera from the three selected cores collected in the eastern Indian Ocean allowed the reconstruction of the palaeoceanographic evolution of the region for up to the last 60 kyrs. The benthic foraminifera fauna, BFAR, the accumulation rate of three selected taxa (*B. aculeata*, *E. exigua* and *U. proboscidea*) and the $\delta^{13}C$ of *C. wuellerstorfi* were examined. The variations in trends for all the proxies parallel already published palaeoceanographic and palaeoclimatological changes reported for this region.

By means of Factor Analysis (Principal Components), the species whose distribution through time was indicative of past environmental changes were identified. The distribution of these species appeared to be controlled by the co-variance of two principal factors: (1) organic matter availability, and (2) dissolved-oxygen levels at the sea floor. These variables are influenced by processes occurring at the sea surface, such as primary productivity levels and presence/absence of low-salinity water cap, as well as by conditions related to deep oceanic circulation. The increased amount of organic matter at the sea floor and its oxidation cause oxygen depletion. In the presence of a poorly ventilated environment, this oxygen depletion can have an additional impact for the ecosystem at the sea floor. On the other hand, in a scarcely oxygenated environment, organic matter can be better preserved, becoming a longer-term "food" resource for the meiofauna.

Different faunal patterns were also observed at different depths:

(1) below 1800 m, *B. aculeata* and *E. exigua* were correlated with conditions of increased organic matter supply to the sea floor. *C. wuellerstorfi* thrived in oligotrophic conditions. *C. wuellerstorfi* also indicates increased deep-water circulation and increased oxygenation; and
(2) for depths ~1000 m and south of 20°S, *C. wuellerstorfi* implies oligotrophic conditions where reduced amounts of organic matter were laterally advected by active bottom currents. The species *G. subglobosa* and *N. irregularis* were associated with an extreme, low carbon-flux rate and high dissolved-oxygen levels. This last condition relates to an increased influence of AAIW. *U. proboscidea* and *B. robusta* became abundant in the presence of low dissolved-oxygen levels and a more stratified water column.

The $\delta^{13}C$ of *C. wuellerstorfi* confirms the presence of an hydrological front in the Indian Ocean during the LGM: below 1800 m, the $\delta^{13}C$ of *C. wuellerstorfi* followed a pattern similar to the one observed elsewhere in the Indian Ocean, showing a depletion >0.32‰ during that time. This indicates for the LGM conditions of reduced deep-water circulation; at ~1000 m, the $\delta^{13}C$ of *C. wuellerstorfi* depletion was <0.32‰. This is in agreement with the isotopic signal recorded from other parts of the Indian Ocean and indicates a more active intermediate-water circulation.

High values of BFAR imply conditions of enhanced organic matter supply to the sea floor. The accumulation rates of *B. aculeata*, *E. exigua* and *U. proboscidea* identify periods characterised by increased organic matter supply and reduced oxygen levels (*U. proboscidea*). These observations point to important differences between the present situation of the eastern Indian Ocean and the past. As indicated above, the $\delta^{13}C$ of *C. wuellerstorfi* appeared to be controlled by intermediate- and deep-water circulation. Our results imply more active circulation for intermediate depths (~1000 m) and reduced circulation below 1800 m during the LGM. Conditions of more/less active circulation controlled dissolved-oxygen levels, thus affecting the benthic foraminiferal fauna.

During the LGM, off the west coast of Western Australia, productivity did not increase. This is indicated by: (a) a benthic foraminiferal assemblage dominated by *G. subglobosa* and *N. irregularis*, (b) the $\delta^{13}C$ of *C. wuellerstorfi* depletion, which was lower than the one expected for this period, and (c) the BFAR pattern, which was characterised by values similar to those of today. This scenario results from more arid conditions on adjacent landmasses, thus causing a reduced amount of nutrients injected into the ocean by rivers, and a steric southward-flow of water along the Australian coast.

Today, the occurrence of *N. irregularis* mirrors the distribution of AAIW in the eastern Indian Ocean and porcellaneous taxa are correlated with low salinity at the sea surface and high dissolved oxygen levels. The high percentages of these taxa recorded off the west coast of Western Australia imply an increased influence of AAIW at latitudes north of 20°S for the LGM. The replacement of the assemblage dominated by *N. irregularis* and *G. subglobosa* by the assemblage dominated by *U. proboscidea* and *B. robusta*, at ~5 kyr BP, relates to an increased influence of the oxygen-depleted IIW and a more stratified water column, due to the presence of the Leeuwin Current.

The productivity of the Banda Sea was higher during the past as suggested the by the high BFAR and high percentages of *B. aculeata*. This species was also favoured by the oxidation of organic matter and a reduced deep-water circulation as seen by low values of $\delta^{13}C$ of *C. wuellerstorfi*, resulting from low dissolved-oxygen level conditions at the sea floor.

Acknowledgements

We wish to thank Judith Shelley, Joe Cali and Arne Sturm (Leibnitz Institute for Marine Sciences, Germany) for their enormous help in sample preparation and isotope analyses. Also, Alexander Altenbach's comments proved of great help in the preparation of the interpretation of the results. We are grateful to Dr. F. Guichard who made the SHI9016 core available for this study. The SHIVA cruise was sponsored by the Laboratoire des sciences du climat through INSU-CNRS with the technical support of GENAVIR-IFREMER. Thanks are also due to K. Hardjawidjaksana, co-chief scientist and Captain Handoko and his crew. The cruise was facilitated by the French Foreign Ministry under a French-Indonesian cooperation. We are grateful to Dr. L. Maeda (JAMETEC Kochi Institute for Core Sample Research) for making the results presented in her PhD thesis. The Australian Research Council and the ANU Faculties Research funds awarded to PDD financed part of the Franklin cruises and isotopic analyses. Some of the AMS dates were provided by ANSTO staff under AINSE grant 97/057R awarded to PDD. The main research was conducted during the tenure of an IPRS scholarship awarded to DSM. We wish to thank the anonymous reviewers as well as Professor T. Corrège for very useful comments made on the original manuscript and for their suggestions which helped improve the text and the interpretation of our data.

Appendix A. Supplementary data

Supplementary data associated with this article can be found, in the online version, at doi:10.1016/j.palaeo.2006.11.002.

References

Adams, J.M., Faure, H., Faure-Dernard, L., McGlade, J.M., Woodward, F.I., 1990. Increases in carbon storage from the Last Glacial Maximum to the present. Nature 348, 711–714.

Ahmad, S.M., Guichard, F., Hardjawidjaksana, K., Adisaputra, M.K., Labeyrie, L.D., 1995. Late Quaternary paleoceanography of the Banda Sea. Marine Geology 122, 385–397.

Altenbach, A.V., 1992. Short term processes and patterns in the foraminiferal response to organic flux rates. Marine Micropaleontology 19, 119–129.

Altenbach, A.V., Pflaumann, U., Ralph, S., Thies, A., Timm, S., Trauth, M., 1999. Scaling and distributional patterns of benthic foraminifera with flux rates of organic carbon. Journal of Foraminiferal Research 29, 173–185.

Barker, R.W., 1960. Taxonomic notes on the species figured by H. B. Brady in his Report on the foraminifera dredged by H.M.S. Challenger during years 1873–1876. Society of Economic Paleontologists and Mineralogists. Special Publication, vol. 9, pp. 1–238.

Barmawidjaja, B.M., Rohling, E.J., van der Kaars, S., Vergnaud Grazzini, C., Zachariasse, W.J., 1993. Glacial condition in the Northern Molucca Sea region (Indonesia). Palaeogeography Palaeoclimatology Palaeoecology 101, 147–167.

Burke, S.K., Berger, W.H., Coulburn, W.T., Vincent, E., 1993. Benthic Foraminifera in box core ERDC 112, Ontong Java Plateau. Journal of Foraminiferal Research 23, 19–39.

Chappell, J., Omura, A., Esat, T., McCulloch, M., Pandolfi, J., Ota, Y., Pillans, B., 1996. Reconciliation of late quaternary sea levels derived from coral terraces at Huon Peninsula with deep sea oxygen isotope records. Earth and Planetary Science Letters 141, 227–236.

Collins, L.S., 1989. Relationships of environmental gradients to morphologic variation within *Bulimina aculeata* and *Bulimina marginata*, Gulf of Maine area. Journal of Foraminiferal Research 19, 222–234.

Corliss, B.H., 1979. Recent deep-sea benthic foraminiferal distributions in the Southeast Indian ocean: inferred bottom water routes and ecological implications. Marine Geology 31, 115–138.

Curry, W.B., Duplessy, J.-C., Labeyrie, L.D., Shackleton, N.J., 1988. Changes in the distribution of the $\delta^{13}C$ of deep water CO_2 between the last glaciation and the Holocene. Paleoceanography 3, 317–341.

De Deckker, P., 2001. Records of environmental changes in the Australian sector of Pep II Point to broad trends of climate change. PAGES Newsletter 9, 4–5.

De Deckker, P., Tapper, N.J., van der Kaars, S., 2002. The status of the Indo-Pacific Warm Pool and adjacent land at the Last Galcial Maximum. Global and Planetary Change 35, 25–35.

den Dulk, M., 2000. Benthic foraminiferal response to Late Quaternary Variations in Surface Water Productivity and Oxygenation in the Northern Arabian Sea. Universiteit Utrecht, Utrecht. 205 pp.

Denne, R.A., Sen Gupta, B.K., 1991. Association of bathyal foraminifera with water masses in the northwestern Gulf of Mexico. Marine Micropaleontology 17, 173–193.

Duplessy, J.-C., Shackleton, N.J., Matthews, K.R., Prell, W., Ruddiman, W.F., Carlap, M., Hendy, C.H., 1984. $\delta^{13}C$ record of benthic foraminifera in the last interglacial ocean: implications for the carbon cycle and the global deep water circulation. Quaternary Research 21, 225–243.

Duplessy, J.-C., Shackleton, N.J., Fairbanks, R.G., Labeyrie, L., Oppo, D., Kallel, N., 1988. Deepwater source variations during the last climate cycle and their impact on the global deepwater circulation. Paleoceanography 3, 343–360.

Duplessy, J.C., Labeyrie, L., Kallel, N., Julliet-Leclerc, A., 1989. Intermediate and deep water characteristics during the last glacial maximum. In: Berger, A., Schneider, S., Duplessy, J.C. (Eds.), Climate and Geo-Science. Kluwer Academic Publisher, Boston, pp. 105–120.

Ellis, B.R., Messina, A.R., 1940. Catalogue of Foraminifera, vol. 13. American Museum of Natural History.

Fieux, M., Andrie, C., Delecluse, P., Ilahude, A.G., Kartavtseff, A., Mantisi, F., Molcard, R., Swallow, J.C., 1994. Measurement within the Pacific-Indian Ocean throughflow region. Deep-Sea Research I 41, 1091–1130.

Fieux, M., Andrie, C., Charriaud, E., Ilahude, A.G., Metzl, N., Molcard, R., Swallow, J.C., 1996. Hydrological and chlorofluoromethane of the Indonesian throughflow entering the Indian Ocean. Journal of Geophysical Research 101, 12,433–12,454.

Gingele, F., De Deckker, P., Hillebrand, C.-D., 2001. Late Quaternary fluctuations of the Leeuwin current and palaeoclimates on the adjacent land masses—clay mineral evidence. Australian Journal of Earth Sciences 48, 1–8.

Gingele, F.X., De Deckker, P., Girault, A., Guichard, F., 2002. High-resolution history of the South Java current during the past 80 Ka. Palaeogeography, Palaeoclimatology, Palaeoecology 183, 247–260.

Gordon, A.L., Fine, R.A., 1996. Pathways of water between the Pacific and Indian Oceans in the Indonesian Seas. Nature 379, 146–149.

Herguera, J.C., Berger, W.H., 1991. Paleoproductivity from benthic foraminifera abundance: glacial to postglacial change in the West-Equatorial Pacific. Geology 19, 1173–1176.

Herguera, J.C., Jansen, E., Berger, W.H., 1992. Evidence for a bathyal front at 2000 m depth in the Glacial Pacific, based on a depth transect on Ontong Java Plateau. Paleoceanography 7, 273–288.

Hess, S., 1998. Distribution patterns of recent benthic foraminifera in the South of China. Berichte Reports, vol. 91. Geol.-Paläont. Inst. Univ. Kiel, Kiel. 173 pp.

Jannink, N.T., Zachariasse, W.J., Van der Zwaan, G.J., 1998. Living (Rose Bengal-stained) benthic foraminifera from the Pakistan continental margin (northern Arabian Sea). Deep-Sea Research I 45, 1483–1513.

Kallel, N., Labeyrie, L., Julliet-Leclerc, D., Duplessy, J.-C., 1988. A deep hydrological front between intermediate and deep water masses in the glacial Indian Ocean. Nature 333, 651–655.

Lutze, G.F., Coulbourn, W.T., 1983. Recent benthic foraminifera from the continental margin of Northwest Africa: community structure and distribution. Marine Micropaleontology 8, 361–401.

Mackensen, A., Sejrup, H.P., Jansen, E., 1985. The distribution of living benthic foraminifera on the continental slope and rise off Southwest Norway. Marine Micropaleontology 9, 275–306.

Mackensen, A., Futterer, D.K., Grobe, H., Schmiedl, G., 1993. Benthic foraminiferal assemblages from the eastern South Atlantic Polar Front region between 35° and 57° S. Marine Micropaleontology 22, 33–69.

Maeda, L., 2003. Interaction between global climate changes and fluctuations of palaeoceanography in the Indo-Pacific Warm Pool during the Late Quaternary. PhD Thesis, Sendai, 131 pp.

Martinez, J.I., De Deckker, P., Chivas, A.R., 1997. New estimates for salinity changes in the Western Pacific Warm Pool during the last glacial maximum—oxygen-isotope evidence. Marine Micropaleontology 32, 311–340.

Martinez, I.J., Taylor, L., De Deckker, P., Barrows, T.T., 1998a. Planktonic foraminifera from the eastern Indian Ocean: distribution and ecology in relation of the Western Pacific Warm Pool (WPWP). Marine Micropaleontology 34, 121–151.

Martinez, J.I., De Deckker, P., Barrows, T.T., 1998b. Palaeoceanography of the western Pacific Warm Pool during the Last Glacial Maximum—of significance to long-term climatic monitoring of the maritime continents. In: Bishop, P., Kershaw, A.P., Tapper, N. (Eds.), Environmental and Human History and Dynamics of the Australian Southeast Asian Region. Catena Verlag.

Martinez, J.I., De Deckker, P., Barrows, T.T., 1999. Palaeoceanography of the last glacial maximum in the eastern Indian Ocean: planktonic foraminiferal evidence. Palaeogeography, Palaeoclimatology, Palaeoecology 147, 73–99.

Martinson, D.G., Pisias, N.G., Hays, J.D., Imbrie, J., Moore, T.C., Shackleton, N.J., 1987. Age dating the Orbital Theory of the Ice Ages: development of a high-resolution 0 to 300,000 chronostratigraphy. Quaternary Research 27, 1–29.

McCorkle, D.C., Veeh, H.H., Heggie, T.H., 1994. Glacial–Holocene paleoproductivity off western Australia: a comparison of proxy records. In: Zahn, R., Pedersen, T.F., Kaminski, M.A., Labeyrie, L. (Eds.), Carbon Cycling in the Glacial Ocean: Constrains on the Ocean's Role in Global Change. NATO ASI Series. Springer-Verlag, Berlin Heidelberg, pp. 443–479.

McCorkle, D.C., Heggie, D.T., Veeh, H.H., 1998. Glacial and Holocene stable isotope distributions in the southeastern Indian Ocean. Paleoceanography 13, 20–34.

Miao, Q.M., Thunell, R.C., 1993. Recent deep-sea benthic foraminiferal distributions in the South China and Sulu Seas. Marine Micropaleontology 22, 1–32.

Miao, Q.M., Thunell, R.C., 1996. Late Pleistocene-Holocene distribution of deep-sea benthic foraminifera in the South China sea and Sulu sea - palaeoceanographic implications. Journal of Foraminiferal Research 26, 9–23.

Murgese, D.S., 2003. Late Quaternary palaeoceanography of the eastern Indian Ocean based on benthic foraminifera. PhD Thesis, Australian National University, Canberra, 177 pp.

Murgese, D.S., De Deckker, P., 2005. The distribution of deep-sea benthic foraminifera in core tops from the eastern Indian Ocean. Marine Micropaleontology 56, 25–49.

Murray, J.W., 1991. Ecology and Palaeoecology of Benthic Foraminifera. Longman Scientific and Technical, Harlow, Essex, England. 397 pp.

Naqvi, W.A., Charles, C.D., Fairbanks, R.G., 1994. Carbon and oxygen isotopic records of benthic foraminifera from the Northeast Indian Ocean: implications on glacial–interglacial atmospheric CO_2 changes. Earth and Planetary Science Letters 121, 99–110.

Okada, H., Wells, P., 1997. Late Quaternary nannofossil indicators of climate change in two deep-sea cores associated with the Leeuwin Current off Western Australia. Palaeogeography Palaeoclimatology Palaeoecology 131, 413–432.

Olley, J.M., De Deckker, P., Roberts, R.G., Fifield, L.K., Yoshida, H., Hancock, G., 2004. Optical dating of deep-sea sediments using single grains of quartz: comparison with radiocarbon. Sedimentary Geology 169, 175–189.

Paillard, D., Labeyrie, L., Yiou, P., 1996. Macintosh program performs time-series analysis. Eos. Trans. AGU 77, 379.

Pearce, A.F., 1991. Eastern boundary currents of the southern hemisphere. Journal of the Royal Society of Western Australia 74, 35–45.

Phleger, F.B., Parker, F.L., Peirson, J.F., 1953. North Atlantic foraminifera. Report of the Swedish Deep-Sea Expedition, vol. 7, pp. 1–122.

Prell, W.P., Hutson, W.H., Williams, D.F., Be, A.W.H., Geitzenauer, K., Molfino, B., 1980. Surface circulation of the Indian Ocean during the last glacial maximum, approximatively 18,000 yr B.P. Quaternary Research 14, 309–336.

Rathburn, A.E., Corliss, B.H., 1994. The ecology of living (stained) deep-sea benthic foraminifera from the Sulu Sea. Paleoceanography 9, 87–150.

Rutberg, R.L., Hemming, S.R., Goldstein, S.L., 2000. Reduced North Atlantic Deep Water flux to the glacial Southern Ocean inferred from neodymium isotope ratios. Nature 405, 935–938.

Sarnthein, M., Winn, K., Duplessy, J.-C., Fontugne, M.R., 1988. Global variations of surface ocean productivity in low and mid latitudes: influence on CO_2 reservoirs of the deep ocean and atmosphere during the last 21,000 years. Paleoceanography 3, 361–399.

Sen Gupta, B.K., Machain-Castillo, M.L., 1993. Benthic foraminifera in oxygen poor habitats. Marine Micropaleontology 20, 183–201.

Shackelton, N.J., 1977. $\delta^{13}C$ in *Uvigerina*: tropical rainforest history and the equatorial Pacific carbonate dissolution. In: Anderson, N., Malahof, A. (Eds.), Fate of Fossil Fuel CO_2 in the Oceans. Plenum, New York.

Spooner, M.I., Barrows, T.T., De Deckker, P., Paterne, M., 2005. Palaeoceanography of the Banda Sea, and Late Pleistocene Initiation of the Northwest Monsoon. Global and Planetary Change 49, 28–46.

Takahashi, K., Okada, H., 2000. The paleoceanography for the last 30,000 years in the southeastern Indian Ocean by means of calcareous nannofossils. Marine Micropaleontology 40, 83–103.

Tomczak, M., Godfrey, J.S., 1994. Regional Oceanography: An Introduction. Pergamon, London. 422 pp.

van der Kaars, W.A., 1991. Palynology of eastern Indonesian marine piston-cores: a Late Quaternary vegetational and climatic record of Australasia. Palaeogeography, Palaeoclimatology, Palaeoecology 85, 239–302.

van der Kaars, W.A., Dam, M.A.C., 1995. A 135,000-year record of vegetational and climatic change from the Bandung area, West-Java, Indonesia. Palaeogeography, Palaeoclimatology, Palaeoecology 117, 55–72.

van der Kaars, S., Dam, R., 1997. Vegetation and climate change in West-Java, Indonesia during the last 135,000 years. Quaternary International 37, 67–71.

van der Kaars, S., De Deckker, P., 2002. A Late Quaternary pollen record from deep-sea core Fr10/95 GC17 offshore Cape Range Peninsula, northwestern Australia. Review of Palaeobotany and Palynology 120, 17–39.

van der Kaars, S., De Deckker, P., Gingele, F.X., 2006. A 100,000 year record of annual and seasonal rainfall and temperature for northwestern Australia based on a marine pollen record. Journal of Quaternary Science 21, 879–889.

Van Marle, L.J., 1988. Bathymetric distribution of benthic foraminifera on the Australia–Irian Jaya continental margin, eastern Indonesia. Marine Micropaleontology 13, 97–152.

Van Marle, L.J., 1989. Recent and fossil benthic foraminifera and Late Cenozoic paleobathymetry of Seram, eastern Indonesia. Netherlands Journal of Sea Research 24, 445–457.

Veeh, H.H., McCorkle, D.C., Heggie, D.T., 2000. Glacial/Interglacial variations of sedimentation on the West Australian continental margin: constrain from excess ^{230}Th. Marine Geology 166, 11–30.

Wells, P.E., Wells, G.M., 1994. Large-scale reorganization of ocean currents offshore Western Australia during the late quaternary. Marine Micropaleontology 24, 157–186.

Wells, P., Wells, G., Cali, J., Chivas, A.R., 1994. Response of deep-sea benthic foraminifera to Late Quaternary climate changes, southeast Indian Ocean, offshore Western Australia. Marine Micropaleontology 23, 185–229.

Wijffels, S.E., Nan, B., Hautala, S., Meyers, G., Morawitz, W.M.L., 1996. The WOCE Indonesian throughflow repeat hydrography sections: I10 and IR6. International WOCE Newsletter 24, 25–28.

Wijffels, S., Sprintall, J., Fieux, M., Bray, N., 2002. The JADE and WOCE I10/IR6 throughflow sections in the southeast Indian Ocean: Part 1. Water mass distribution and variability. Deep-Sea Research II 49, 1341–1362.

Williams, C.B., 1964. Patterns in the Balance of Nature. Academic Press, London. 324 pp.

Wyrtki, K., 1958. The water exchange between the Pacific and the Indian Oceans in relation to upwelling processes. Oceanography 16, 61–65.

Wyrtki, K., 1962. The upwelling in the region between Java and Australia during the southeast monsoon. Australian Journal of Marine and Freshwater Research 12, 217–225.